

ENGINEERING RESEARCH JOURNAL (ERJ)

Volume (54) Issue (2) April. 2025, pp:268-279 https://erjsh.journals.ekb.eg

Behavior of GFRP HPC- Columns Exposed to Axial Load and Elevated Temperature

Ahmed Mohammed Helal * 1; Taha A. El-Sayed 1; Yousry B. Shaheen 2

- ¹Department of Civil Engineering, Faculty of Engineering at Shoubra, Benha University, Cairo, Egypt.
- ²Department of Civil Engineering, Faculty of Engineering, Menoufia University, Menoufia, Egypt.

E-mail: ahmed.hilal 19@feng.bu.edu.eg; taha.ibrahim@feng.bu.edu.eg; ybishaheen@gmail.com.

Abstract: This study examines the combined impact of axial load and elevated temperature (up to 300 °C) on concrete columns reinforced by GFRP. The study suggests an economical and accurate method for evaluating the fire resistance of these columns under external load and elevated temperatures. The experiment was conducted on 8 samples casted from normal and high-strength concrete. The normal concrete has a 30 MPa strength and a water-cement ratio of 42%, while the high-strength concrete has a strength of 60MPa and a water to cement ratio of 25%, and a silica fume ratio of 15%. The tested concrete column samples have dimensions of 150 mm in depth, 150 mm in breadth and 1500 mm in height. The laboratory experiment was conducted and the column was subjected to axial load while the column was exposed to elevated temperature (300 °C). The study variables included concrete strength and the sequence of thermal and mechanical loading (before, during, or after heating). Although previous studies examined either the thermal degradation of GFRP bars or the structural performance of concrete columns under fire, few studies combined both aspects under realistic loading conditions. The findings indicate that GFRP-reinforced columns experience noticeable reductions in load capacity and ductility under elevated temperatures, particularly when heating occurs before loading. High-strength concrete columns showed better residual strength and deformation control than normal-strength ones.

Keywords: HPCC, Axial Load, Temperature Development, HSCC, GFRP, NSC, NSCC.

1. INTRODUCTION

Recently, the construction industry has been moving to protect facilities from exposure to harsh conditions. Fires causing high temperatures result in structural performance degradation, by deteriorating the structural elements and possibly causing collapse. Therefore, researches have been done widely on improving the strength of the concrete elements to high temperatures and preventing structural failure [1-3]. Notably, El-Sayed [1] has contributed by developing a patented method for evaluating the behavior of reinforced concrete elements under elevated temperatures, offering valuable insights for engineers designing such structures. A critical issue encountered when concrete is exposed to elevated temperatures is the alteration of the

physical and mechanical properties of steel reinforcement. Therefore, studies have explored replacing steel reinforcement with alternative materials, such as fiberglass bars, which maintain their properties at higher temperatures [2-6]. Fiberglass reinforcement provides several advantages, notably its high-temperature resistance and the capability to incorporate a thermal insulating layer, thus preserving its mechanical and physical properties under thermal stress [4-7]. Upon exposure to heat, fiberglass bars undergo visible changes, with their color darkening gradually. At temperatures up to 100°C, fiberglass reinforcement shows negligible effects; however, when temperatures reach around 400°C, significant changes in stress-strain behavior become apparent [5].

^{*} Corresponding Author.

For structures exposed to elevated temperatures, improving concrete properties through additives is advisable. Such additives enhance concrete's physical and mechanical under characteristics high-temperature conditions. substantially reducing structural damage [8-11]. El-Sayed et al. [10] investigated the performance of ultra-highperformance concrete (UHPCC) when subjected to both axial compressive load and high temperatures (600°C). In another study, El-Sayed et al. [12] developed a patented technique for evaluating the behavior of reinforced concrete components under high temperatures, offering valuable insights for engineers designing such structures. These studies have shown that the elevated-temperature behavior of HPC notably differs from that of NSC, potentially compromising fire safety [13-15]. The incorporation of fibers has been examined as a potential solution to mitigate concrete spalling at elevated temperatures. Bangi and Horiguchi [16] investigated the impact of fibers on pore pressure evolution in high-strength concrete (HSC) subjected to heat, identifying that long polypropylene (PP) fibers effectively reduced pore pressure development. Kalifa et al. [17] proved that concrete spalling can be reduced by combining polypropylene fibres with high-performance concrete. Similarly, Xiao and Falkner [18] found that utilizing PP fibers decreased explosive spalling in HPC. However, Varona et al. [19] found that involving steel fibers with high aspect ratios may reduce ductility at elevated temperatures.

Fiber-reinforced polymer (FRP) strengthening has emerged as an effective method for enhancing the structural performance of concrete columns. Glass fiber-reinforced polymer (GFRP) in particular offers significant advantages in improving the axial load capacity, ductility, and energy absorption of reinforced concrete columns through external confinement [20, 21]. The lateral confinement provided by GFRP wrapping can potentially mitigate some of the brittle characteristics exhibited by high-strength concrete members [22, 23]. Numerous studies have concluded that the use of FRP circumferential wraps on the exterior face of RC columns can significantly enhance their strength and ductility. Al-Rousan et al. [24] investigated the axial behavior of CFRP-confined circular reinforced concrete columns and proposed a stress-strain model and practical design guidelines. The application of external FRP wrapping enhances the axial load capacity, ductility, moment resistance, and energy absorption of reinforced concrete (RC) columns. This improvement results from the confinement effect provided by the FRP, which counteracts the lateral expansion of the concrete under axial loads [25-27]. Further studies by Al-Rousan [28] examined the behavior of circular reinforced concrete columns confined with CFRP composites. Research on the rehabilitation of heat-damaged concrete structures using FRP has also shown promising

results. Roy et al. [29] demonstrated that using FRP jackets is an effective technique for restoring structural strength and enhancing the energy dissipation capacity of reinforced concrete short columns subjected to elevated temperatures. Al-Nimry et al. [30] investigated the impact of FRP confinement on circular columns exposed to elevated temperatures. The study revealed that completely encasing the columns with carbon FRP sheets led to notable improvements in both axial load capacity and toughness, while using two layers of GFRP sheets effectively restored the compressive strength of the heat-damaged specimens. Bisby et al. [31] examined concrete cylinders and reported an increase in vertical load-bearing capacity of thermally damaged specimens attributed to CFRP wraps. Al-Salloum et al. [32] examined the effects of diverse elevated temperatures on reinforced concrete circular columns enhanced through various methods. Yaqub et al. [33] noticed that a single layer of GFRP or CFRP sheet enhanced the ultimate strength, ultimate strain, and ductility of post-heated reinforced concrete square columns, though initial stiffness was not improved. Benzaid et al. [34] discovered that the efficacy of GFRP confinement was based on specimen geometry and the number of GFRP layers applied. Despite extensive research on the behavior of HPC and FRP-strengthened columns independently, there remains a knowledge gap regarding the combined performance of GFRP-wrapped HPC columns under simultaneous axial loading and elevated temperature conditions. This study aims to investigate the behavior of GFRP-strengthened HPC columns when subjected to axial loads while exposed to elevated temperatures, with particular focus on structural integrity, load-carrying capacity, and failure mechanisms.

This research contributes to the growing body of knowledge on fire-resistant structural elements and provides valuable insights for the design and implementation of GFRPstrengthened HPC columns in applications where fire safety is a critical consideration.

2. Significance of the Study

- Comparing the behavior of normal-strength and highstrength concrete columns when they are exposed to fire while they are loaded and reinforced with glass fiber bars.
- Studying the effect of elevated temperatures on fiber glass bars while they are loaded
- Providing solutions for elements at risk of high temperatures using alternative materials to traditional materials

3. Analyses of experiments

3.1Utilized Materials

3.1.1Sand:

Sand has a 2.60 specific gravity, 2.4 fineness modulus and unit weight of 1620 kg/m3. The analysis of sieving was carried out following ECP' 203/2020 standards [35].

3.1.2 Coarse aggregate:

The coarse aggregate exhibited a unit weight of 1600 kg/m³ and a maximum nominal size of 10 mm. Its water absorption capacity remained below the allowable limit of 2.5%, complying with the specifications outlined in ECP 203/2020 standards [35].

3.1.3 Cement:

Specific gravity = 3.15 Cement type CEM I 42.5 N and CEM I 52.5 N meeting the requirements of E.S. 262/1988, was used in high-strength concrete. [36]

3.1.4 Water:

In the mixing and drying steps, clean tap water was used, which doesn't contain any impurities.

3.1.5 Superplasticizer:

Superplasticizer with density 1.1kg/Liter. It is mainly used to produce self-levelling concrete with only the water necessary to fully hydrate the cement particles. The super-plasticizer used was ADDICRETE BVF, which is a product of chemical for Modern Building Company.

3.1.6 GFRP RFT:

Diameter 8mm for stirrup, and deformed bars of diameter 12mm [35].

3.1.7 Silica fume :

Silica-fume was utilized as a partial substitute for cement (10% cement weight) to improve the mortar strength as much as feasible. It was supplied in the form of a fine powder with a typical grayish appearance. The selected substitution was picked according to research findings. The chemical composition of silica fume is mainly dominated by silicon dioxide (SiO₂), which makes up about 92-94% of the material. This high percentage of silica is what gives the material its strong pozzolanic properties, allowing it to react efficiently with cement components and improve the strength and durability of mortar. In addition to silica, silica fume contains a small amount of carbon (3-5%), which may slightly affect its color and performance. Other compounds such as iron oxide, calcium oxide, aluminum oxide, magnesium oxide, and traces of potassium, sodium, and manganese oxides are present in very small quantities. These minor components have a limited but sometimes beneficial role in the chemical reactions within cementitious mixtures.

Overall, the composition confirms that silica fume is a fine and reactive material, well-suited for enhancing mortar and concrete properties.

Tabel 2 shows the chemical makeup of silica fumes.

Chemical	Weight%
SiO2	92–94
Carbon	3–5
Fe2O3	0.1-0.5
Cao	0.1-0.15
AL2O3	0.2-0.3
MgO	0.1-0.2
Man O	0.008
K2O	0.1
Na2O	0.1

3.2 Columns Preparation

The experiment tested 8 NSCC and HPCC with a 15% silica cement ratio and a 0.25 water-to-binder ratio. **Error! Reference source not found.** presents the utilized mixtures, while 0outlines the variables taken into consideration, including loading conditions. Oindicates the details of the specimen.

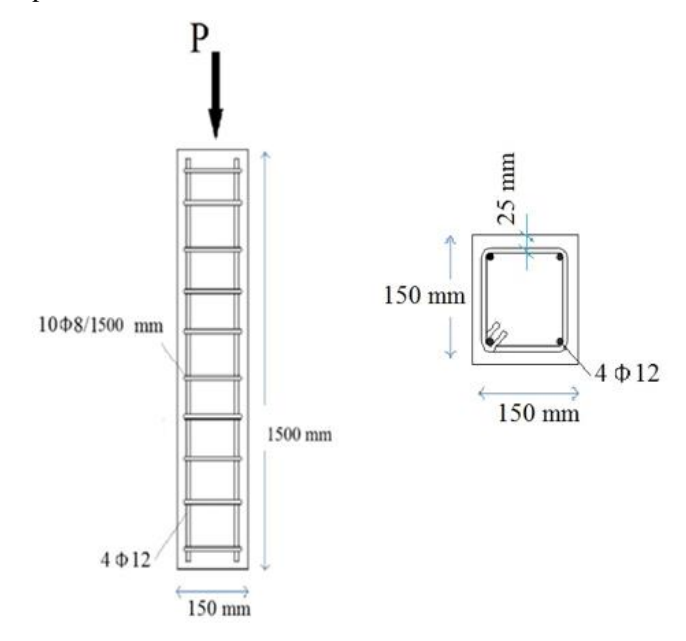


Fig 1.Tested Columns Reinforcement Details

TABLE I. MIX DESIGN

Mix ID	Cement kg/m³	Coarse aggregate kg/m³	Sand kg/m³	Water kg/m ³	W/C	S/C	Superplastizer kg/m³	28days f _{cu} (MPa)	f _t (MPa)
Мо	400	1100	700	170	42.5		3	30	2.55
M1	500	1330	495	125	0.25	15	20	60	5.1

TABEL III DETAILS OF TESTED COLUMNS

Groups	Column ID	RFT.Type	Long.RFT.	Trans.RFT
	C1-A	GFRP	4φ12	φ8@166.67
GROUP A	C2-A	GFRP	4φ12	φ8@166.67
GROUP A	C3-A	GFRP	4φ12	φ8@166.67
	C4-A	GFRP	4φ12	φ8@166.67
GROUP B	C1-B	GFRP	4φ12	φ8@166.67
	C2-B	GFRP	4φ12	φ8@166.67
	С3-В	GFRP	4φ12	φ8@166.67
	C4-B	GFRP	4φ12	φ8@166.67

TABEL IV DEFINITION OF EXAMINED NSCC AND HPCC

Mix ID	Notation	Definition		
	C1-A	Specimen vertically loaded at ambient temperature and used as a		
		control sample with GFRP reinforcement.		
	C2-A	Specimen exposed to 300°C, then loaded vertically until failure		
Mo	С3-А	Specimen initially loaded to 60% of its failure load, subsequently		
		heated to 300°C, and finally loaded vertically until failure.		
	C4-A	Specimen loaded to 60% of failure load, heated to 300°C, then		
		gradually cooled in air, followed by vertical loading to failure with		
		GFRP reinforcement.		
	C1-B	Specimen vertically loaded at ambient temperature and used as a		
		control sample with GFRP reinforcement.		
	C2-B	Specimen exposed to 300°C, then loaded vertically until failure		
M1	С3-В	Specimen initially loaded to 60% of its failure load, subsequently		
1411		heated to 300°C, and finally loaded vertically until failure.		
	C4-B	Specimen loaded to 60% of failure load, heated to 300°C, then		
		gradually cooled in air, followed by vertical loading to failure with		
		GFRP reinforcement.		

3.3 Test Setup

As mentioned, each mix included 4 Columns, The following are the testing conditions which were considered:

- The axial strength was implemented on the first RC column and the result of this column was taken as a reference
- 2) The second column was heated to 300 $^{\circ}$ C and then tested in the axial strength set-up
- 3) The third RC column was first loaded up to 60 % of the ultimate load as predicted from the designs and then fired up to 300°C and then tested in the axial strength setup
- 4) The fourth loaded by about 60% from its ultimate load and then fired up to 300°C, then cooled in air, followed by tested in the axial strength set-up
- 5) The load-displacement curve was recorded automatically by the computer connected to the

flexural strength test facility and the data were retrieved to be analyzed

It should be noted that the temperature history from the room temperature up to 300°C was recorded for the whole tested columns.

3.4 Techniques of Firing the RC Columns

0and 0 showed the technique of inducing temperature in the tested RC columns. The technique comprised the following:

- Confining the RC columns with an electrical coil which can withstand temperatures up to 1200°c.fixed pitch of 125 mm was used to obtain regular. temperature distribution
- 2) Covering the RC column with an insulating sheet to prevent heat dissipation.
- 3) A hole was created to place the thermocouple and monitor the temperature until it reached 300°C...
- 4) Plugging the electrical plug to raise the coil temperature.
- 5) Recording the temperature gradient using the thermocouple to investigate the influence of the density of concrete on the heat transfer inside the tested area.

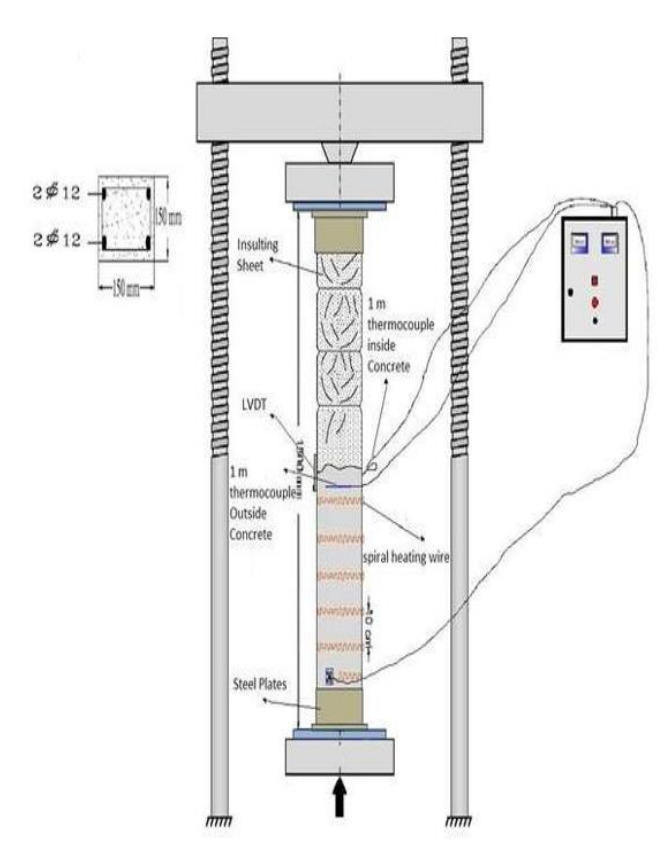


Fig 2 test setup (a)



Fig 3 Test setup(b)

4. RESULTS AND Discussion

4.1 Mixes Strength

0 summarizes the cube compressive strength results for mixes Mo and M1, with cube strengths varying between 30 MPa and 60 MPa. The tensile strength exhibited a similar pattern, reaching up to 5.10 MPa in mix M1.0Shows Concrete Cubes Test. Six cubes with dimensions of $150 \times 150 \times 150$ mm were prepared from each mix to evaluate the concrete compressive strength at 7 and 28 days.

Tabel V	MIXES STREN	IGTH
Mix ID	28days fcu (MPa)	28days ft (MPa)
Мо	30	2.55
M1	60	5.10



Fig 4 Concrete Cubes Test

4.2GFRP Bars

GFRP (Glass Fiber Reinforced Polymer) bars were utilized as stirrups alternative of steel reinforcement because of their resistance to corrosion under different conditions. The tensile strength of GFRP bars is illustrated 0

The tensile capacity of the GFRP bars is depicted in Figure 5. In order to reduce the cost of the bars used in the experimental phase, they were manufactured locally using a design approach resembling widely available skewers. The strength values of these bars ranged from 675 MPa to 750 MPa for bar diameters of 8 mm and 10 mm, respectively, as indicated in TABLE VI. These values were determined through pull-out testing, with results shown in Figure 6.

Summary of Tensile Strength and Corresponding Strain for the Tested GFRP Bars

Bar Dimeter (mm)	Ultimate Tensile strength (Mpa)	Corresponding strain (mm/mm)		
6	600	0.0037		
8	675	0.005		
10	750	0.0049		

4.3Temperature variation at the Specimen's Surface

In 0and Below, temperature variations on the surface and inside of the tested columns can be observed when subjected to both load and heat. The objective of this study was to investigate the behavior of the columns under elevated temperatures during axial loading, specifically aiming for a temperature of 300°C. For the columns in Group A, it was found that column C2-A surpassed the required temperature, reaching 300°C on the outer surface of the concrete in 15 minutes. The internal temperature of this column also increased significantly, reaching 150°C. The remaining columns in Group A, namely C3-A and C4 A, reached the desired temperature within 20 to 35 minutes, with internal temperatures ranging from 170°C to 171°C. Moving on to Group B columns, both C2-B and C3-B achieved the desired temperature of 300°C on the outer surface simultaneously, taking 13 minutes. Internally, C2-B reached 146.02°C, while C3-B reached 107°C. On the other hand, column C4-B took the longest time, requiring 32 minutes to reach 300°C on the outer surface with an internal temperature of 152°C.

4.4 Load carrying capacity

TABLE II. shows the specimen's load-carrying capacities. The results of the experiment demonstrate a decrease in the ultimate load after exposure to elevated temperatures (up to 300°C), when compared with the reference specimens C1-A and C1-B that were not exposed to heat. Columns C1-A and C1-B, considered as control specimens, achieved ultimate loads of 733.21 kN and 1380 kN, respectively. With the impact of elevated temperatures (up to 300°C), columns C2-A, C3-A, and C4-A reached ultimate loads of 689.58 kN,

713.84 kN, and 706.4 kN, which correspond to 94.05%, 97.36%, and 96.35% of the reference C1-A. For the high-strength concrete group (Group B), columns C2-B, C3-B, and C4-B reached 1050 kN, 1125 kN, and 924 kN, which represent 76.09%, 81.52%, and 66.96% of the reference C1-B. The toughness values for control columns were 2591.18 kN.mm for C1-A and 4343.53 kN.mm for C1-B. Comparatively, the toughness values for the tested columns were: C2-A: 1655.57 kN.mm, C3-A: 2017.83 kN.mm, C4-A: 2130.47 kN.mm, C2-B: 1163.26 kN.mm, C3-B: 2976.50 kN.mm, C4-B: 1867.35 kN.mm, C4-A: 2130.47 kN.mm, C2-B: 1163.26 kN.mm, C4-B: 1867.35 kN.mm, C4-B: 1867.35 kN.mm, C4-B: 1867.35 kN.mm, C4-B: 1867.35 kN.mm.

For further clarity, the strain values correspond to the ultimate loads, as shown in 0 and 0 are as follows:C1-A:0.0026 mm/mm,C2-A:0.0014,C3-A:0.0012,C4-A:0.0026mm/mm,C1-B:0.0025mm/mm,C2-B:0.0014, C3-B:0.001 mm/mm,C4-B:0.0015 mm/mm.

The **toughness** was calculated using the **trapezoidal rule**, which estimates the area under the load-displacement curve. This was done by summing the areas of trapezoids formed between consecutive load and displacement points using the following expression.

Toughness =
$$\sum \left[\frac{(P_i + P_{i+1})}{2} \times (\delta_i - \delta_{i+1}) \right]$$

Where P is the load in kN and δ is the corresponding displacement in mm. This method provides a numerical approximation of the energy absorption capacity of the column up to failure.

The results show that high temperatures reduce the load capacity and toughness.

4.5 Crack load and ultimate load

The cracking load (Pcr) was measured for each column when the first visible crack appeared, using an L.V.D.T after removing the insulation and electrical coils. The ultimate load (Pu) was also documented. According to TABLE II., a significant reduction in both the first crack load and ultimate load was observed when fire exposure was introduced. in Group A, the control column C1-A recorded a first crack load of 594.52 kN and an ultimate load of 733.21 kN. The fireexposed columns (C2-A, C3-A, and C4-A) showed decreases in the first crack load by 11.18%, 14.29%, and 7.13%, respectively, and in the ultimate load by 5.95%, 2.64%, and 3.65%, respectively. Similarly, in Group B, the control column C1-B had the highest first crack load at 902 kN and an ultimate load of 1380 kN. The fire-affected columns C2-B, C3-B, and C4 B recorded reductions in the first crack load by 25.61%, 6.67%, and 32.93%, respectively, and in the ultimate load by 23.91%, 18.48%, and 33.04%, respectively.

Based on the results, there was a clear reduction in both the first crack load and the ultimate load when the fire factor element was added to the experiment.

4.6 Load displacement curves

From the plotted load-displacement curves 0and 0 all columns showed elastic behavior up to the first crack, followed by nonlinear plastic deformation until failure. Fire exposure caused a decline in ultimate load, ductility, and toughness. The ultimate load and toughness for column C1-A were 733.21 kN and 2591.18 kN.mm, respectively, while column C1-B recorded 1380 kN and 4343.53 kN.mm. In comparison, the fire-exposed columns showed reduced values: C2-A reached 689.58 kN with a toughness of 1655.57 kN.mm, C3-A recorded 713.84 kN and 2017.83 kN.mm, and C4-A had 706.4 kN with 2130.47 kN.mm. Similarly, columns in Group B showed reductions, with C2-B achieving 1050 kN and 1163.26 kN.mm, C3-B reaching 1125 kN and 2976.50 kN.mm, and C4-B yielding 924 kN with a toughness of 1867.35 kN.mm. These results highlight the significant deterioration in performance due to elevated temperature exposure.

The differences in the results are related to how each column was tested. Columns that were loaded before heating (like C3-A and C3-B) gave better performance than those that were heated first (C2-A and C2-B). The control columns (C1-A and C1-B), which were tested without heating, had the best value because they stayed in their original design condition.

4.6.1 Energy Absorption (Toughness)

Toughness, defined as the area under the load displacement curve, reflects a column's energy absorption capacity. Compared to the control specimen C1-A (2591.18 kN·mm), the toughness of specimens C2-A, C3 A, and C4-A decreased by 36.09%, 22.1%, and 17.8%, respectively. Similarly, when compared to specimen C1-B (4463.35 kN·mm), the toughness of C2-B, C3-B, and C4-B decreased by 73.94%, 33.31%, and 58.15%, respectively. These reductions indicate the detrimental influence of elevated temperatures on the energy absorption capability of the tested columns, particularly evident in C2-B and C2 A.

4.6.2 Ductility Factor

The ductility factor is the ratio of deflection at failure (δu) to deflection at first crack (δy). Compared to specimen C1-A (ductility = 2.20), specimens C2-A and C3-A exhibited increased ductility by 17.27% and 15.91%, respectively. On the other hand, C4-A showed a reduction in ductility of 19.55%. In Group B, and relative to specimen C1-B (ductility = 3.2), the ductility factors for C2-B, C3-B, and C4-B decreased by 29.69%, 51.25%, and 66.15%, respectively. These results highlight the notable reduction in deformation

capacity under thermal exposure, especially in high-strength concrete mixes subjected to elevated temperatures.

4.6.3 Failure modes and crack patterns

One of the most important ways to describe the failure mechanism, understand how the failure happened, and examine the impact of the parameters on the behavior of the tested column is to track the route of cracks and record the associated loads at various loading levels. The crack patterns of the tested columns are shown in 0and 0The fractures in C1-A begin at 148 kN, where the load remains constant and increases gradually to 733.21kN upon reaching its highest level.

For group A, with a normal-strength concrete mix. When specimen C2-A a failure load of 689.58 kN, the first crack appeared and continued to grow in length. There was an 11.17% decrease in the first crack load. There was a 14.3% and 7.1% decrease in the first crack load for specimens C3-A and C4-A, respectively, compared to the control specimen. For group B, with a high-strength concrete mix. When specimen C2-B reached a failure load of 1050 kN, where the load was increased to the maximum. There was a 6.7% and 32.9% decrease in the first crack load for specimens C3-B and C4-B, respectively, compared to the control specimen.

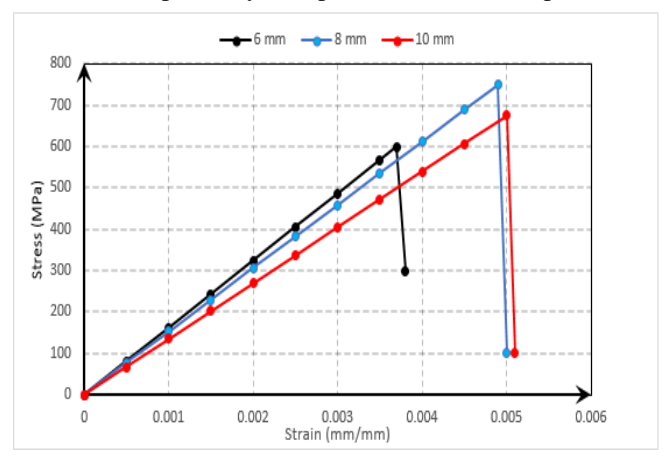


Fig 5 Stress-strain curve for the used GFRP bars.



Fig 6 Failure Mode of GFRP bars.

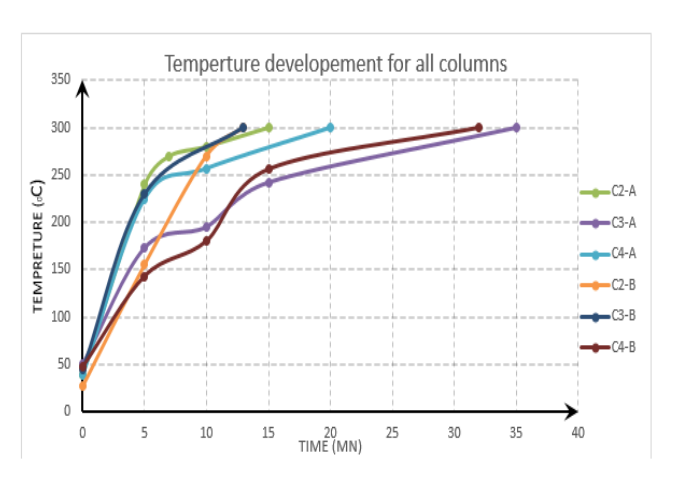


Fig 7 Temperature Development Outside Concrete Columns

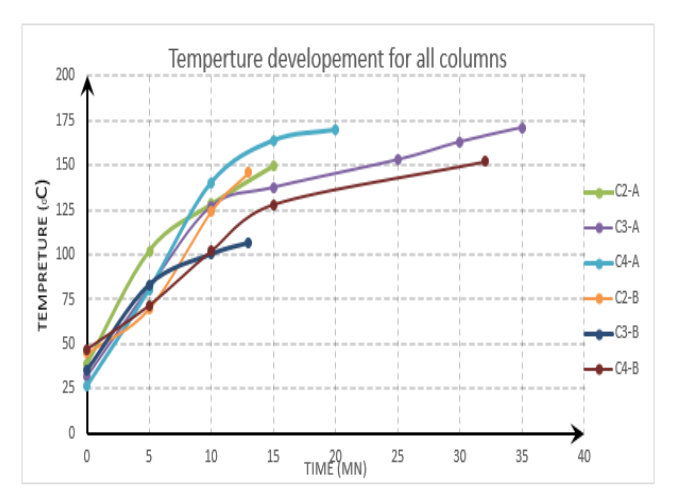


Fig 8 Temperature Development Inside Concrete Columns

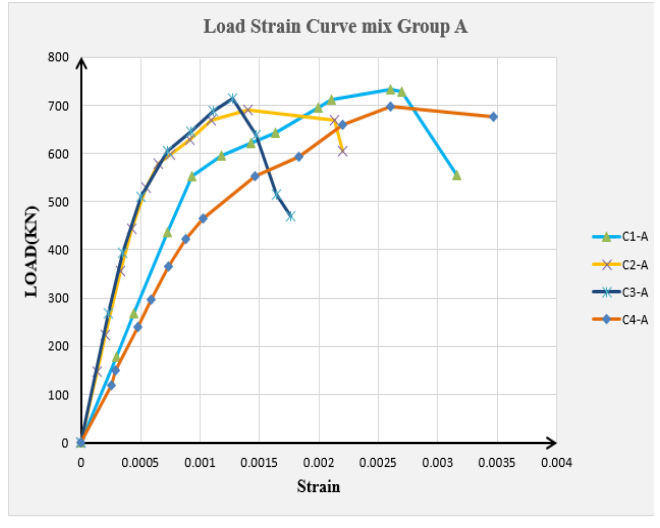


Fig 9 Load strain curves of column C1-A,C2-A,C3-A,C4-A

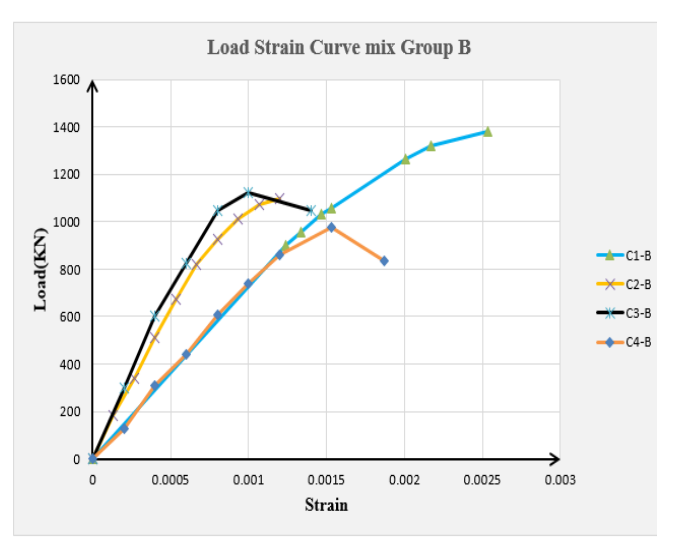
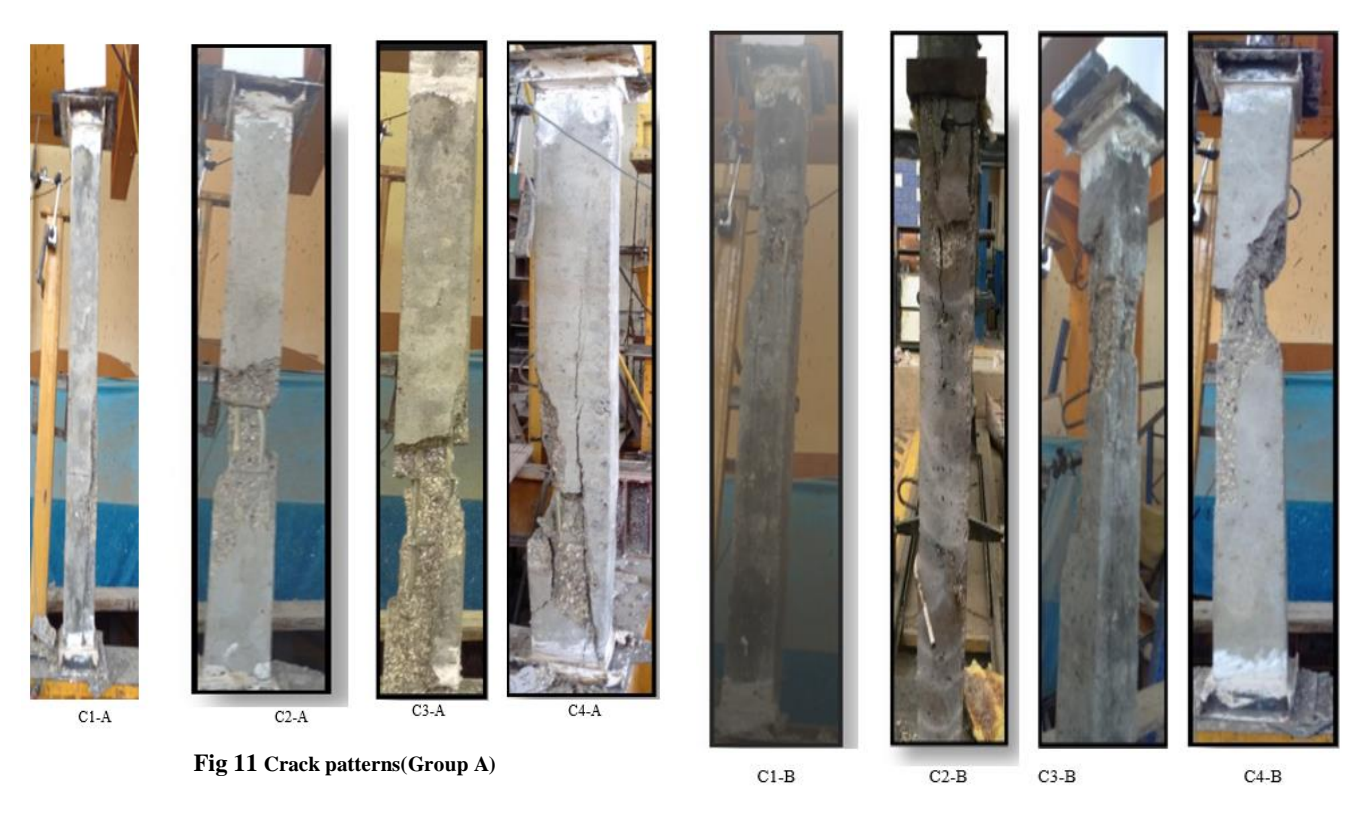
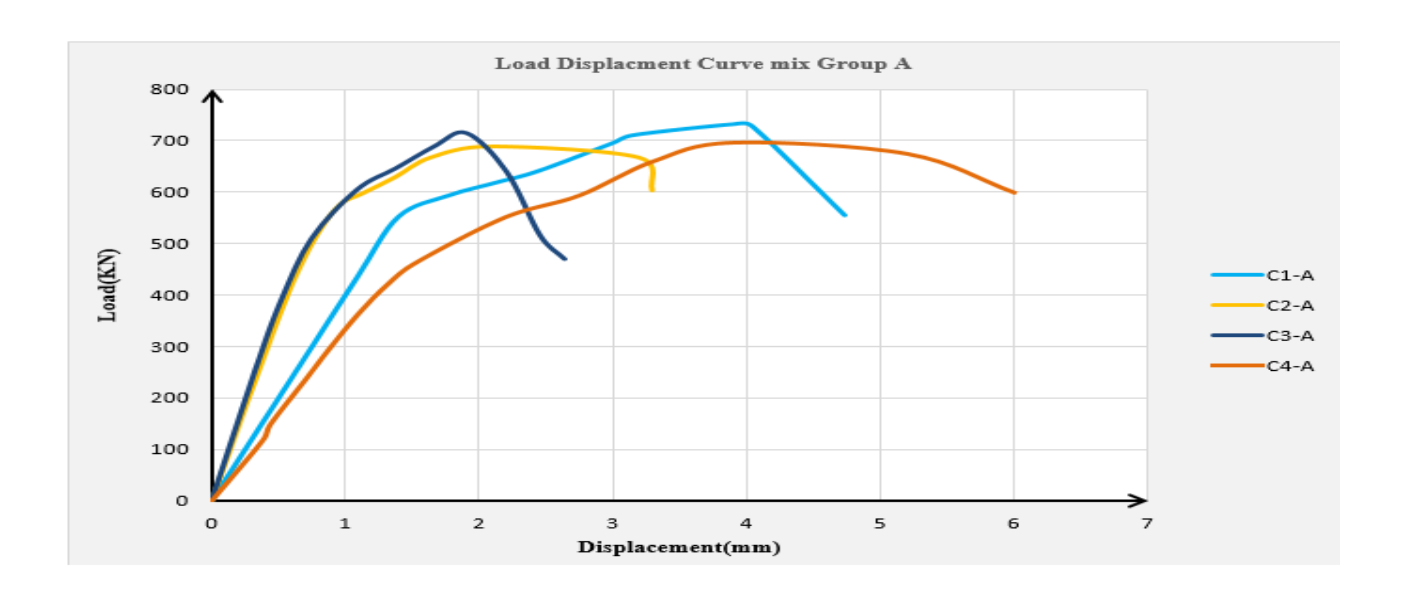


Fig 10 Load strain curves of column C1-B,C2-B,C3-B,C4-B



 $Fig\ 12\ Crack\ patterns (Group\ B)$

		TABLE II. T	EST RESULTS OF I	NSCC & HPC	C	
Column	First crack Load (KN)	Failure load	Deflection At the first crack load (mm)	Def.at Ult. load	Ductility ratio	Toughness (kN.mm)
No		(kN)		(mm)		
C1-A	594.52	733.21	1.77	3.9	2.20	2591.18
C2-A	528.06	689.58	0.815	2.1	2.58	1655.57
С3-А	509.54	713.84	0.75	1.91	2.55	2017.83
C4-A	552.105	706.4	2.2	3.9	1.77	2130.47
C1-B	902	1380	1.86	83.	2.043	4343.53
С2-В	671	1050	0.8	1.8	2.25	1163.26
С3-В	841.82	1125	0.96	1.5	1.56	2976.50
C4-B	605	924	1.2	1.3	1.083	1867.35



FIRST CRACK AND ULTIMATE LOADS OF TESTED COLUMNS .

Column	First Crack	Change in First Crack	Ultimate Load (kN)	
No	KN	Load (%)		Change in Ultimate Load
		` '		(%)
C1-A	594.52	0	733.21	0
C2-A	528.06	-11.18	689.58	-5.951
С3-А	509.54	-14.29	713.84	-2.642
C4-A	552.105	-7.134	706.4	-3.657
C1-B	902	0	1380	0
C2-B	671	-25.61	1050	-23.91
С3-В	841.82	-6.672	1125	-18.48
C4-B	605	-32.93	924	-33.04

Fig 13 Load displacement curves of column C1-A,C2-A,C3-A,C4-A

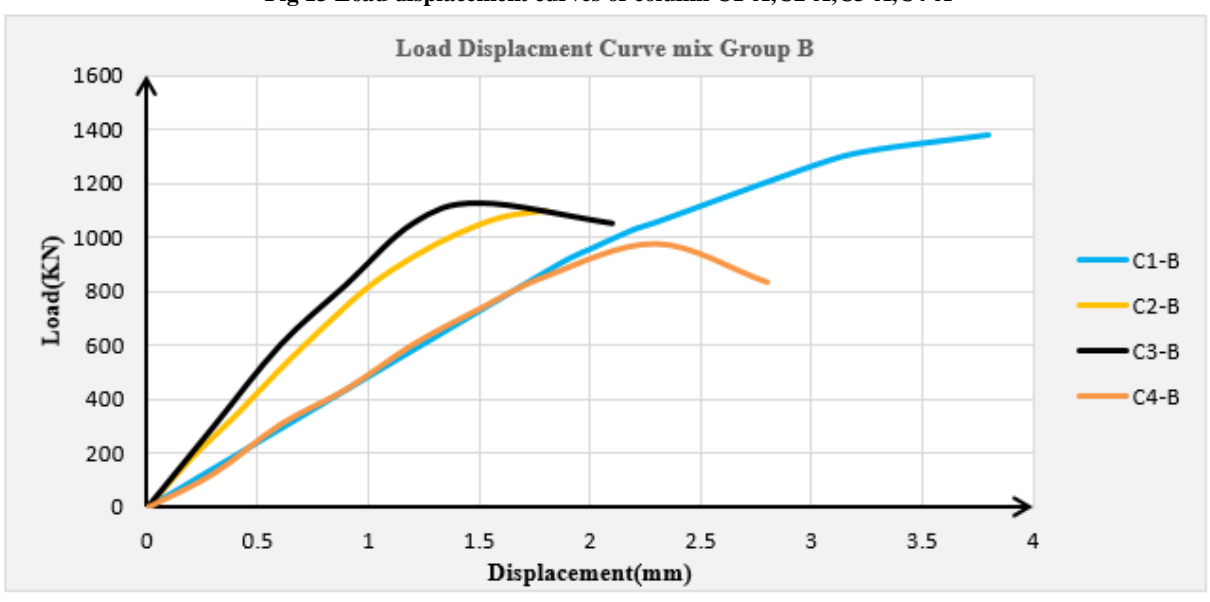


Fig 14 Load displacement curves of column C1-B,C2-B,C3-B,C4-B

4.7 THEORETICAL STUDY

The contribution of glass fiber bars has yet to be fully defined by the CSA [37]. Accurately determining the ultimate load capacity of glass fiber-reinforced concrete (GFRC) columns remains challenging due to the presence of multiple failure mechanisms. As shown in Equation 1, Afifi et al. [38] were essential for the calculation of the cross-sectional area (CS) of glass fiber bars. The compressive strength of glass fiber bars is estimated using Equation 2 based on Tobbi et al.'s [39] linear-elastic theory. Although this model predicts a lower strain level than the test results, it yields a projected load that is lower than the actual load recorded in the research. Equations 3, as calculated by Samani and Attard [40], determine the axial strain values were determined for unconfined concrete cylinders. According to the results in 0, Equations 1 to 3 significantly underestimated the axial load capacity for the specimens of group A. However, for group B columns, Equation 4 produced values that closely matched the experimental loads, offering the most reliable predictions for glass fiber-reinforced concrete (GFRC) columns under elevated load conditions.

$$P_N = kc \times fc \times (Ag - A_{FRP}) + 0.35 \times fu_{FRP} \times A_{FRP}$$
 (1)

$$P_N = kc \times fc \times (Ag - A_{FRP}) + 0.002 \times E_{FRP} \times A_{FRP}$$
 (2)

$$P_N = kc \times fc \times (Ag - A_{FRP}) + 0.0025 \times E_{FRP} \times A_{FRP}$$
 (3)

$$P_P = Ac \, Pck + As \, Psk \tag{4}$$

Where:

 P_N = the nominal axial load capacity

kc =the ratio between the in-place strength to concrete cylinder strength (usually 0.85 for concrete)

fc = compressive strength of concrete (MPa)

 $Ag = \text{gross cross-sectional area of the concrete section (mm}^2)$ $A_{FRP} = \text{cross-sectional area of the GFRP reinforcement bars (mm}^2)$

EVALUATION OF EXPERIMENTAL RESULTS AGAINST THEORETICAL PREDICTIONS

Column ID	Exp. Load (kN)	Eq. (1)	Eq. (2)	Eq. (3)	Eq. (4)
C1-A	733.21	782	476	571	552
C2-A	689.58	782	476	571	552
С3-А	713.84	782	476	571	552
C4-A	706.4	782	476	571	552
C1-B	1380	1282	906	1071	1052
C2-B	1050	1282	906	1071	1052
С3-В	1125	1282	906	1071	1052
C4-B	979	1282	906	1071	1052

 fu_{FRP} = ultimate tensile strength of the GFRP bars (MPa)

 P_{sk} = Contribution of reinforcement bars

As= refers to the total cross-sectional area of the longitudinal GFRP reinforcement bars in the column

As= refers to the total cross-sectional area of the longitudinal GFRP reinforcement bars in the column.

The constants 0.35, 0.002, and 0.0025 used in Equations (1)–(3) represent estimated contributions of GFRP bars under compression or assumed strain limits based on previous It's important to mention that Equations (1) to (4) were created based on tests at normal room temperature, so they don't include the effects of high temperatures on materials

5.CONCLUSION

Based on the experimental and analytical investigation conducted in this study on GFRP-reinforced concrete columns exposed to elevated temperatures and axial loads, the following conclusions can be drawn:

- Elevated temperature significantly reduced the loadcarrying capacity of GFRP-reinforced columns, especially when the heat exposure occurred before applying the axial load. This reduction was more pronounced in normal-strength concrete than in high-strength concrete.
- High-strength concrete (HSC) columns exhibited better residual performance under thermal loading conditions. They showed higher toughness, lower deformation, and better crack control compared to normal-strength concrete columns.
- 3. The energy absorption capacity (toughness) decreased notably in all heated specimens. The reduction in toughness was more critical in HSC columns subjected to early thermal exposure, indicating the sensitivity of GFRP bars to heat.
- 4. The load-displacement behavior of all columns showed a clear shift from elastic to plastic response, followed by brittle failure in heated specimens. Fire exposure reduced ductility and stiffness, highlighting the importance of considering thermal effects in design.
- 5. The crack patterns and failure modes varied depending on the heating sequence, with earlier exposure resulting in more pronounced cracks and premature failure. This finding emphasizes the role of thermal load history on structural performance.
- The theoretical predictions using traditional models underestimated the actual load capacities, especially for normal-strength concrete. This suggests the need for improved models that account for the behavior of GFRP-reinforced concrete under fire.
- 7. Using GFRP bars offers a lightweight, corrosion-resistant alternative to steel, but they still require protective strategies against fire. Incorporating high-strength concrete improves the overall resistance and stability under extreme conditions.

REFERENCES

- El-Sayed T. A. (2019). A Method for Testing Reinforced Concrete Elements Under Elevated Temperature. Egyptian Patent No. 29493. Issued November 11, 2019.
- [2]. El-Sayed, T.A., Erfan, A.M., Abdelnaby, R.M. and Soliman, M.K., 2022. Flexural behavior of HSC beams reinforced by hybrid GFRP bars with steel wires. Case Studies in Construction Materials, 16, p.e01054.
- [3]. Ostrowski, K., M. Dudek, and Ł. Sadowski, Compressive behaviour of concrete-filled carbon fiber-reinforced polymer steel composite tube columns made of high performance concrete. Composite Structures, 2020. 234: p. 111668.
- [4]. Erfan, A.M., Abd Elnaby, R.M., Badr, A.A. and El-sayed, T.A., 2021. Flexural behavior of HSC one way slabs reinforced with basalt FRP bars. Case Studies in Construction Materials, 14, p.e00513.
- [5]. Yoo, S.W. and J.F. Choo, Behavior of CFRP-reinforced concrete columns at elevated temperatures. Construction and Building Materials, 2022. 358: p. 129425.
- [6]. El-Sayed, T.A., 2019. Flexural behavior of RC beams containing recycled industrial wastes as steel fibers. Construction and Building Materials, 212, pp.27-38.
- [7]. Erfan, A.M., Hassan, H.E., Hatab, K.M. and El-Sayed, T.A., 2020. The flexural behavior of nano concrete and high strength concrete using GFRP. Construction and Building Materials, 247, p.118664.
- [8]. Erfan, A.M., Algash, Y.A. and El-Sayed, T.A., 2019. Experimental & analytical flexural behavior of concrete beams reinforced with basalt fiber reinforced polymers bars. Int. J. Sci. Eng. Res., 10(8), pp.297-315.
- [9]. Aslam, F., AbdelMongy, M., Alzara, M., Ibrahim, T., Deifalla, A.F. and Yosri, A.M., 2022. Two-Way Shear Resistance of FRP Reinforced-Concrete Slabs: Data and a Comparative Study. Polymers, 14(18), p.3799.
- [10]. El-Sayed, T.A., Abdallah, K.S., Ahmed, H.E. and El-Afandy, T.H., 2023. Structural behavior of ultra-high strength concrete columns reinforced with basalt bars under axial loading. International Journal of Concrete Structures and Materials, 17(1), p.43.
- [11]. Erfan, A.M., Algashb, Y.A. and El-Sayed, T.A., 2019. Experimental and Analytical Behavior of HSC Columns Reinforced with Basalt FRP Bars. Int. J. Sci. Eng. Res., 10(9), pp.240-260.
- [12]. El-Sayed, T.A., A.-R.M. Youssef, and A.S. Shanour, The Behavior of Ferrocement RC Beams Exposed to Flexural Load and Elevated Temperature. Engineering Research Journal (Shoubra), 2024. 53(3): p. 137-154.
- [13]. Cheng, F.-P., V. Kodur, and T.-C. Wang, Stress-strain curves for high strength concrete at elevated temperatures. Journal of Materials in Civil Engineering, 2004. 16(1): p. 84-90.
- [14]. Kodur, V., et al., Effect of strength and fiber reinforcement on fire resistance of high-strength concrete columns. Journal of Structural Engineering, 2003. 129(2): p. 253-259.
- [15] Kodur, V. and R. McGrath. Performance of high strength concrete columns under severe fire conditions. in Proceedings Third International Conference on Concrete under Severe Conditions, Vancouver, BC, Canada. 2001.
- [16]. Bangi, M.R. and T. Horiguchi, Effect of fibre type and geometry on maximum pore pressures in fibre-reinforced high strength concrete at elevated temperatures. Cement and Concrete Research, 2012. 42(2): p. 459-466.
- [17]. Kalifa, P., G. Chene, and C. Galle, High-temperature behaviour of HPC with polypropylene fibres: From spalling to microstructure. Cement and concrete research, 2001. 31(10): p. 1487-1499.
- [18]. Xiao, J. and H. Falkner, On residual strength of high-performance concrete with and without polypropylene fibres at elevated temperatures. Fire safety journal, 2006. 41(2): p. 115-121.
- [19]. Varona, F., et al., Influence of high temperature on the mechanical properties of hybrid fibre reinforced normal and high strength concrete. Construction and Building Materials, 2018. 159: p. 73-82.
- [20] Hasan, H.A., Sheikh, M.N., & Hadi, M.N.S. (2017). Experimental Investigation of Circular High-Strength Concrete Columns Reinforced with Glass Fiber-Reinforced Polymer Bars and Helices under Different Loading Conditions. Journal of Composites for Construction, 21(4), 04017005..
- [21]. Al-Salloum, Y.A., Influence of edge sharpness on the strength of square concrete columns confined with FRP composite laminates. Composites Part B: Engineering, 2007. 38(5-6): p. 640-650.

- [22]. Al-Rousan, R.Z. and M.H. Barfed, Impact of curvature type on the behavior of slender reinforced concrete rectangular column confined with CFRP composite. Composites Part B: Engineering, 2019. 173: p. 106939.
- [23]. Cao, Y.-G., Jiang, C., & Wu, Y.-F. (2016). Cross-Sectional Unification on the Stress-Strain Model of Concrete Subjected to High Passive Confinement by Fiber-Reinforced Polymer. Polymers, 8(5), 186.
- [24]. Al Rousan, R.Z. and M.A. Issa, Stress-strain model and design guidelines for CFRP - confined circular reinforced concrete columns. Polymer Composites, 2018. 39(8): p. 2722-2733.
- [25]. Abdalla, K.M., et al., Finite-element modelling of concrete-filled steel tube columns wrapped with CFRP. Proceedings of the Institution of Civil Engineers-Structures and Buildings, 2020. 173(11): p. 844-857.
- [26]. Benzaid, R., Mesbah, H., & Chikh, N. (2010). FRP-confined concrete cylinders: axial compression experiments and strength model. Materials and Structures, 43(9), 1241–1253..
- [27] Issa, M.A., R.Z. Alrousan, and M.A. Issa, Experimental and parametric study of circular short columns confined with CFRP composites. Journal of Composites for Construction, 2009. 13(2): p. 135-147.
- [28]. Al-Rousan, R., Behavior of circular reinforced concrete columns confined with CFRP composites. Procedia Manufacturing, 2020. 44: p. 623-630.
- [29]. Roy, A., U. Sharma, and P. Bhargava, Strengthening of heat damaged reinforced concrete short columns. Journal of Structural Fire Engineering, 2014. 5(4): p. 381-398.
- [30]. Al-Nimry, H.S. and A.M. Ghanem, FRP Confinement of Heat-Damaged Circular RC Columns. International Journal of Concrete Structures and Materials, 2017. 11(1): p. 115-133.
- [31] Bisby, L.A., et al., Strengthening fire-damaged concrete by confinement with fibre-reinforced polymer wraps. Engineering Structures, 2011. 33(12): p. 3381-3391.
- [32]. Al-Salloum, Y.A., H.M. Elsanadedy, and A.A. Abadel, Behavior of FRP-confined concrete after high temperature exposure. Construction and Building Materials, 2011. 25(2): p. 838-850.
- [33] Yaqub, M. and C.G. Bailey, Repair of fire damaged circular reinforced concrete columns with FRP composites. Construction and Building Materials, 2011. 25(1): p. 359-370.
- [34]. Benzaid, R., N.-E. Chikh, and H. Mesbah, Behaviour of Square Concrete Column Confined with Gfrp Composite Warp/Kompozitiniais Stiklo PluoŠtu Armuoto Polimero LakŠtais SustiprintŲ KvadratiniŲ BetoniniŲ KolonŲ Elgsena. Journal of Civil Engineering and Management, 2008. 14(2): p. 115-120.
- [35] ESS 203-2020 (2020), Egyptian Standard Specifications for the Design and Construction of Reinforced Concrete Structures, Ministry of Housing and Urban Communities, Cairo, Egypt.
- [36]. Housing and Building National Research Center (HBRC). (1988). Egyptian Code for Design and Construction of Reinforced Concrete Structures (E.S. 262/1988). Cairo, Egypt.
- [37]. Faruqi, M., et al., Research and design guidelines for the construction of fiber-reinforced polymer reinforced concrete structures under fire exposure: A brief review. Journal of Reinforced Plastics and Composites, 2013. 32(17): p. 1302-1309.
- [38]. Afifi, M.Z., H.M. Mohamed, and B. Benmokrane, Axial capacity of circular concrete columns reinforced with GFRP bars and spirals. Journal of Composites for Construction, 2014. 18(1): p. 04013017.
- [39]. Tobbi, H., A.S. Farghaly, and B. Benmokrane, Concrete Columns Reinforced Longitudinally and Transversally with Glass Fiber-Reinforced Polymer Bars. ACI Structural Journal, 2012. 109(4).
- [40]. Samani, A.K. and M.M. Attard, A stress-strain model for uniaxial and confined concrete under compression. Engineering Structures, 2012. 41: p. 335-3.